

## Reviewed Preprint

Published from the original preprint after peer review and assessment by eLife.

## About eLife's process

## Reviewed preprint posted

July 11, 2023 (this version)

## Posted to bioRxiv

June 6, 2023

## Sent for peer review

May 3, 2023

# Spatial Transcriptomics of Meningeal Inflammation Reveals Variable Penetrance of Inflammatory Gene Signatures into Adjacent Brain Parenchyma

Sachin P. Gadani, Saumitra Singh, Sophia Kim, Matthew D. Smith, Peter A. Calabresi, Pavan Bhargava 

Division of Neuroimmunology, Department of Neurology, Johns Hopkins University School of Medicine, Baltimore, MD, USA • Solomon Snyder, Department of Neuroscience Johns Hopkins University School of Medicine, Baltimore, MD, USA

 ([https://en.wikipedia.org/wiki/Open\\_access](https://en.wikipedia.org/wiki/Open_access))

 (<https://creativecommons.org/licenses/by/4.0/>)

## Abstract

While modern high efficacy disease modifying therapies have revolutionized the treatment of relapsing-remitting multiple sclerosis, they are less effective at controlling progressive forms of the disease. Meningeal inflammation is a recognized risk factor for cortical grey matter pathology which can result in disabling symptoms such as cognitive impairment and depression, but the mechanisms linking meningeal inflammation and grey matter pathology remain unclear. Here, we performed MRI-guided spatial transcriptomics in a mouse model of autoimmune meningeal inflammation to characterize the transcriptional signature in areas of meningeal inflammation and the underlying brain parenchyma. We found broadly increased activity of inflammatory signaling pathways at sites of meningeal inflammation, but only a subset of these pathways active in the adjacent brain parenchyma. Sub-clustering of regions adjacent to meningeal inflammation revealed the subset of immune programs induced in brain parenchyma, notably the B cell mediated immune response and antigen processing/presentation. Trajectory gene and gene set modeling analysis confirmed variable penetration of immune signatures originating from meningeal inflammation into the adjacent brain tissue. This work contributes a valuable data resource to the field, provides the first detailed spatial transcriptomic characterization in a model of meningeal inflammation, and highlights several candidate pathways in the pathogenesis of grey matter pathology.

### eLife assessment

Brain inflammation is a hallmark of multiple sclerosis. Using novel spatial transcriptomics methods, the authors provide **convincing** evidence for a gradient of immune genes and inflammatory markers from the meninges toward the adjacent brain parenchyma in a mouse model. This **important** study advances our understanding of the mechanisms of brain damage in this autoimmune disease.

## Introduction

Multiple sclerosis (MS) is a chronic autoimmune disease of the central nervous system (CNS) characterized by a relapsing remitting and/or progressive course of demyelination, axonal injury, and neurologic dysfunction<sup>1</sup>. Highly efficacious disease modifying therapies have revolutionized the prevention and treatment of MS relapses, but are less effective at stopping hallmarks of MS progression such as brain atrophy<sup>2</sup>. Accumulating evidence points to a pivotal role for leptomeningeal inflammation (LMI) in contributing to this pathology<sup>3, 4</sup>. LMI is found in all subtypes of MS, ranging histologically from disorganized collections of leukocytes to highly organized ectopic lymphoid follicles, and correlates with the presence of cortical grey matter demyelination, neurite loss, and decreased volume<sup>5</sup>. Grey matter pathology (GMP) has been linked to debilitating symptoms such as cognitive impairment and depression<sup>6</sup>, and tends to occur in spatial relation to areas of LMI. Indeed, the most common grey matter lesion location is directly sub-pial<sup>7</sup>, and there is a gradient of increased pathology towards the surface of the brain in MS patients<sup>8, 9</sup>. Interestingly, GMP occurs without local blood-brain barrier disruption or robust infiltration of peripheral immune cells into the brain parenchyma<sup>10, 11</sup>. LMI is therefore speculated to be a source of pro-inflammatory molecules that contribute to GMP<sup>12</sup>, but the pathway(s) involved remain unknown.

Several putative mechanisms linking LMI to GMP have been proposed. Magliozzi and colleagues identified increased expression of numerous cytokines and chemokines, including interferon gamma (IFN $\gamma$ ), tumor necrosis factor (TNF), interleukin (IL)-2, IL-22, CXCL13, and CXCL10, in the meninges and CSF of postmortem MS cases with high levels of meningeal inflammation and GM demyelination<sup>13</sup>. Microarray analysis of cortical lesions from MS cases with LMI revealed a shift in TNF signaling from TNFR1/TNFR2 and NF $\kappa$ B-mediated anti-apoptotic pathways towards TNFR1- and RIPK3-mediated pro-apoptotic/pro-necroptotic pathways<sup>14</sup>. In marmoset and rat models of experimental autoimmune encephalomyelitis (EAE), sub-pial cortical lesions were found with prominent microglial activation and immunoglobulin deposition on myelin sheaths<sup>15, 16</sup>. Interestingly, complement deposition, one possible mechanism of immunoglobulin-related cellular injury, is not found in purely cortical grey matter lesions, in contrast to white or grey/white matter lesions<sup>17</sup>. Numerous other mediators of injury, including reactive oxygen and nitrogen species, metabolic stress, and excitotoxicity have been proposed to drive neurodegeneration in MS and may be at play in GMP.

Previous attempts to characterize the relation between LMI and GMP have been limited by the absence of spatially resolved data, which therefore lacks critical information about the anatomic relationship between LMI and the underlying brain parenchyma. Here, we present a spatial transcriptomic dataset and analysis in a mouse model of relapsing/remitting CNS autoimmunity and meningeal inflammation, Swiss Jim Lambert (SJL) mouse EAE<sup>18</sup>. Our prior work in SJL EAE demonstrated meningeal areas of gadolinium contrast enhancement on magnetic resonance imaging (MRI) that correspond histologically to collections of B cells, T cells, and myeloid cells<sup>19</sup>. In the parenchyma adjacent to areas of meningeal inflammation we identified astrogliosis, activated microglia, demyelination and evidence of axonal stress and damage<sup>19</sup>. This work characterizes the spatially resolved transcriptome of LMI in the SJL EAE model system, revealing the subset of genes and gene sets active in the LMI that extend into the adjacent parenchyma and providing insights into immune pathways that could underlie sub-pial neurodegeneration.

## Materials and methods

### Animals

SJL/J mice were purchased from Jackson Laboratories for all experiments. All mice were maintained in a federally approved animal facility at Johns Hopkins University in accordance with the Institutional Animal Care and Use Committee. Female mice aged 7–8 weeks were used in all experiments and were housed in the animal facility for at least 1 week prior to the start of experiments.

### Induction of SJL EAE

Female SJL/J mice were immunized subcutaneously at two sites over the lateral abdomen with 100 µg PLP139-151 peptide with complete Freund's adjuvant containing 4 µg/ml *Mycobacterium tuberculosis* H37RA (Difco Laboratories). Mice were weighed and scored serially to document disease course. Scoring was performed using the following scale: 0, normal; 1, limp tail; 2, hind limb weakness; 3, hind limb paralysis; 4, hind limb and forelimb weakness; and 5, death.

### MRI imaging

At weeks 6, 8, and 10 post immunization, a horizontal 11.7 T scanner (Bruker BioSpin) with a triple-axis gradient system (maximum gradient strength = 740 mT/m), 72 mm volume transmit coil and 4-channel receive-only phased array coil was used to image the mouse forebrain. During imaging, mice were anaesthetized with isoflurane together with mixed air and oxygen (3:1 ratio) and respiration was monitored via a pressure sensor and maintained at 60 breaths/min. Before imaging, 0.1 ml diluted Magnevist® (gadopentetate dimeglumine, Bayer HealthCare LLC, 1:10 with PBS) was injected. Scans were then analyzed to identify areas of meningeal contrast enhancement by two independent examiners (P.B., S.K.). We counted the number of areas of meningeal contrast enhancement on each individual MRI slice and used the cumulative number to represent the amount of meningeal contrast enhancement. All quantifications were performed by at least two independent examiners and their scores were averaged.

### Tissue preparation and spatial gene expression assay

At 12 weeks post-immunization, animals were euthanized in CO<sub>2</sub> chamber and perfused with cold PBS. Brains were dissected and one hemisphere drop fixed in isopentane cooled on dry ice. Fresh frozen brain samples were then cut coronally at a thickness of 10 µm and placed on the capture area of Visium Gene Expression slides (v1; 10x Genomics). Each slide contained four 6.5 mm x 6.5 mm capture areas. Sample preparation was carried out according to manufacturer's instructions. After fixation with methanol at -20°C, Hematoxylin and Eosin (H&E) staining was performed for morphological analysis and spatial alignment of the sequencing data. After the enzymatic permeabilization, mRNA was captured by probes and cDNA generated. Barcoded cDNA was isolated using SPRIselect-cleanup (Beckman Coulter) and amplified. Amplified cDNA was fragmented and subjected to end-repair, poly-A-tailing, adaptor ligation, and 10x-specific sample indexing as per the manufacturer's instructions. Following assessment of RNA quality, sequencing was performed using a Novaseq S2 100. Brains from four naïve and four EAE mice were used to prepare 5 and 6 individual samples per group, respectively.

## Spatial transcriptomics data processing

Each sample went through identical quality control processing steps. SpaceRanger software (v.1.3.1) was used to pre-process the sequencing data, aligning to the mm10-2020A reference transcriptome. Feature barcoded expression matrixes were used as input for downstream spatial transcriptomics analysis using Seurat (v.4.3.0) and SPATA2 (v.0.1.0)<sup>20</sup>. Data was loaded and analyzed using the Seurat, and all spots that were determined to not be over tissue were discarded using the `filter.matrix` option in Seurat's `Load10XSpatial` function. Spots with less than 250 measured genes and less than 500 unique molecular identifiers (UMIs) were filtered out. Data normalization and stabilization of sequence depth variance was performed on each sample using SCTransform with default parameters<sup>21</sup>. Sample data was then annotated and combined into a merged object for downstream quality control and analysis. Dimensionality reduction was performed using principal component analysis (PCA), followed by computation of shared nearest neighbors of the first 10 principal components and cluster identification (resolution 0.3). To visualize all spots in a two-dimensional plot, a UMAP was created with Seurat's `RunUMAP` function using the first 10 principal components. Cluster and sub-cluster enriched genes were identified with Wilcoxon tests as implemented in the `FindMarkers` function within Seurat. Differential gene expression between groups was attained using DESeq2 (v.1.38.2) on samples pseudobulked by biological replicate. Gene set enrichment analysis and visualization was performed using the gene ontology database<sup>22, 23</sup> and the clusterProfiler package (v.4.6.0)<sup>24</sup>. Estimated signaling pathway activities were calculated for each spot with the top 500 genes of each pathway on SCTransformed data using the PROGENy package (v.1.20.0)<sup>25</sup>. For subclustering analysis, select clusters were subsetted before undergoing dimensionality reduction, neighbor calculation, cluster identification, marker identification, and gene set enrichment as described above. Trajectory gene and gene set modeling analysis was performed with the SPATA2 package.

## Statistics and data visualization

Plots were generated and statistics calculated using R (v.4.2.2) and Rstudio (v.2022.07.2). Bar plots, box plots, MA plots, Venn diagram, and dot plots were produced with ggplot2 (v.3.4.0); heat maps were produced with pHeatmap (v.1.0.12); spatial feature plots and dimensionality reduction plots were produced with Seurat; tree plots were produced with clusterProfiler, and trajectory heatmaps were produced with SPATA2.

All reported P-values adjusted for multiple comparisons were corrected using the Benjamini-Hochberg method<sup>26</sup> unless otherwise specified. The number of samples in the EAE and naïve groups was chosen based on expected levels of variability in prior experiments.

## Results

We tracked the development of LMI during SJL EAE using contrast enhanced serial MRI imaging. MRI data was then used to target areas of LMI for spatial transcriptomics (Figure 1A). Mice developed a characteristic relapsing pattern of neurologic impairment, and contrast-enhanced MRI was performed at weeks 6, 8, and 10 post immunization (Figure 1B-C). In the SJL EAE model, contrast enhancing meningeal lesions are most frequently found in the intrapeduncular cistern, quadrigeminal cistern, and the cleft between the hippocampus and medial geniculate nucleus<sup>19, 27</sup> (Figure 1D). Lesion number remained stable throughout the disease course independent of EAE score (Supplemental Figures 1A-B).

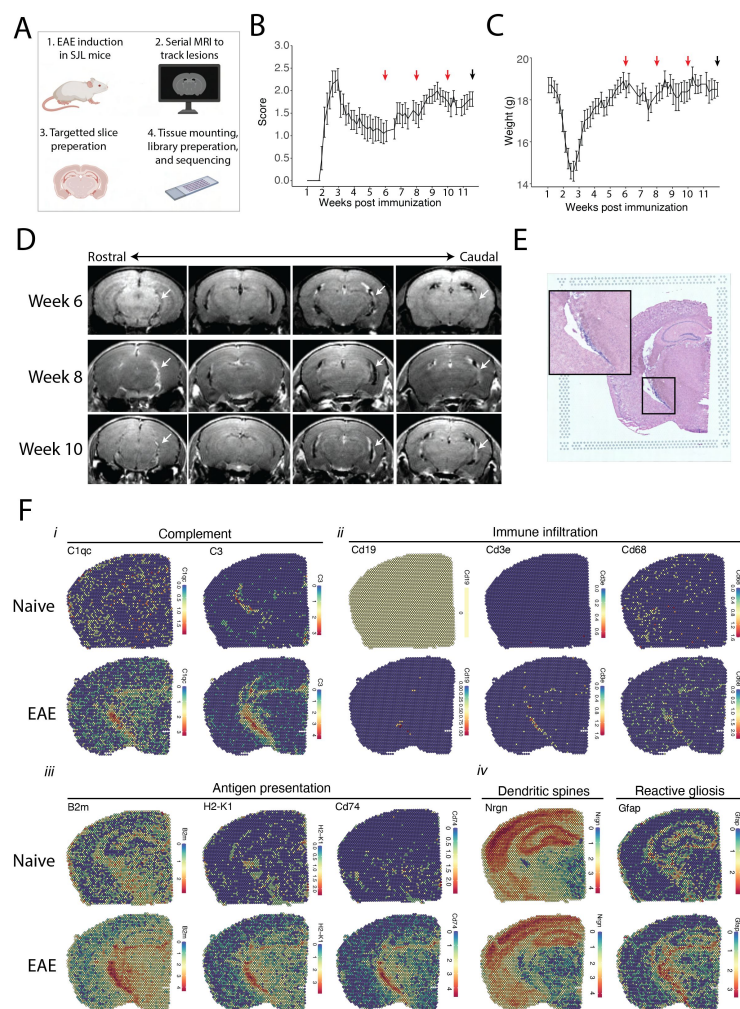


**Figure 1:**

## MRI guided spatial transcriptomics of meningeal-based inflammation in SJL EAE.

(A) Schematic describing the experimental paradigm. SJL mice underwent brain MRI 6-, 8-, and 10- weeks post immunization with MOG 35-55. Brain slices from regions with meningeal inflammation were collected and processed for spatial transcriptomics on the 10x Genomics platform. (B–C) Behavior scores (B) and mouse weights (C) of the EAE cohort. Red arrows indicate MRI time points, black arrow indicates time of tissue harvesting (N = 6). (D) Representative post-contrast MRI brain images, white arrows indicate areas of meningeal-based inflammation. (E) Representative image of H&E-stained tissue section mounted on spatial transcriptomics slide. (F) Spatial feature plots from naïve (top row) and EAE (bottom row) representative samples demonstrate altered expression of genes related to complement (i), immune infiltration (ii), antigen presentation (iii), dendritic spines, and astrocyte activation (iv).

Brain slices were collected from four naïve mice and four EAE mice 11 weeks post-immunization and used to prepare five and six samples for spatial transcriptomics, respectively. H&E staining confirmed the presence of meningeal inflammation in the areas of contrast enhancement, as we had previously observed<sup>19</sup> (Figure 1E). Data from all samples were of high quality and read depth when assessed by treatment group (Supplemental Figure 2A–C) or sample (Supplemental Figure 2D–E). There was expected anatomic variability in number of read counts and number of features per spot, with relatively low counts and features in white matter as compared to the cortex or hippocampus (Supplemental Figure 2F–G), and spots had similar degrees of average complexity between EAE and naïve samples (Supplemental Figure 2H). UMAP clustering revealed no significant independent effect of sample (Supplemental Figure 2I) or slide (Supplemental Figure 2J). Numerous genes were differentially expressed between EAE and naïve slices as estimated by DESeq2 on samples pseudobulked by biological replicate (Supplementary Table 1; Supplemental Figure 2K), including genes associated with the complement cascade, immune infiltration, antigen presentation, and astrocyte activation (Figure 1F).

We next explored the activity of a broad range of pathways using the pathway responsive genes (PROGENy) method<sup>25</sup> (Figure 2A). Inflammatory pathways related to TNF, JAK-STAT, and NFκB signaling were upregulated in EAE compared to naïve, with peak activity around sites of meningeal inflammation (Figure 2B–C). Pathways related to Trail and PI3K were downregulated in EAE compared to naïve (Figure 2D–E), and TGFβ pathway activity was unchanged between groups (Figure 2D–E).



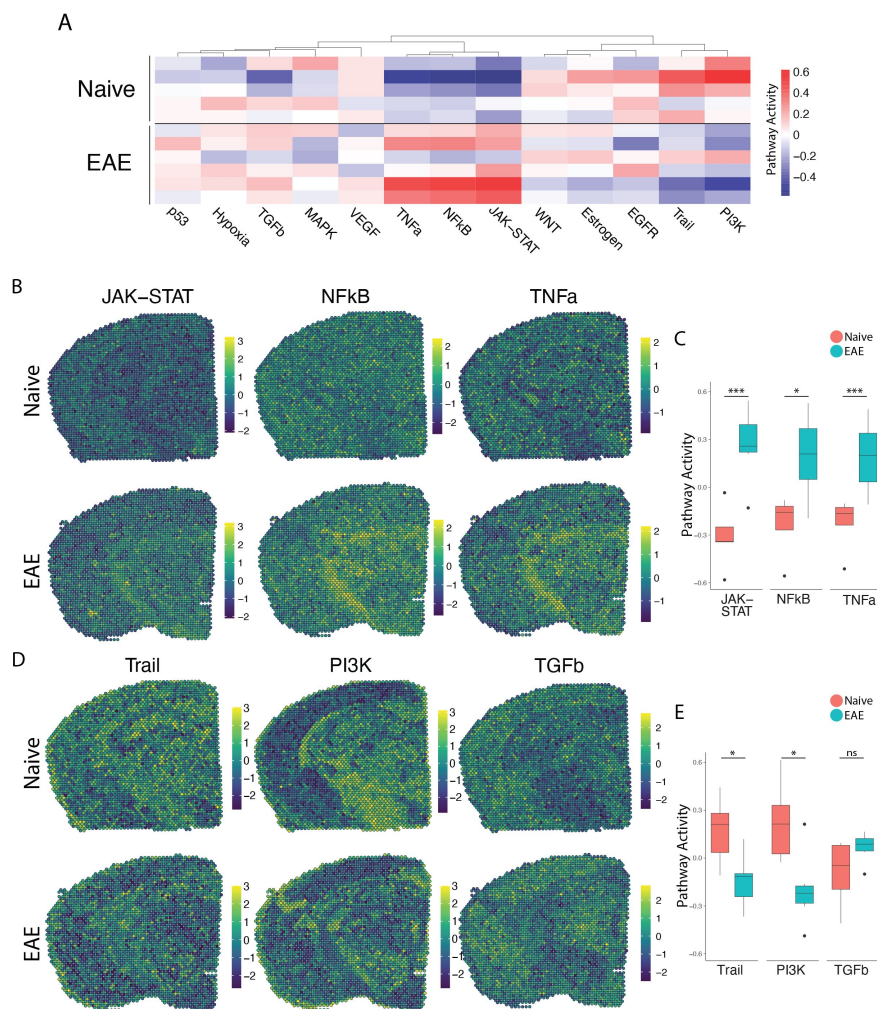


**Figure 2**

## PROGENy analysis reveals spatially restricted pathway activity differences between naïve and EAE.

(A–B) Heat map displaying averaged PROGENy pathway analysis results. (C) Representative spatial plot showing activity of the JAK-STAT, NFkB, and TNFa signaling pathways. (D) Comparison of JAK-STAT, NFkB, and TNFa pathway activities between groups. (E) Representative spatial plot showing activity of the Trail, PI3K, and TGFb signaling pathways. (F) Comparison of Trail, PI3K, and TGFb pathway activities between groups. (Naïve mouse N = 4, sample N = 5; EAE mouse N = 4, sample N = 6; multiple T tests corrected for multiple comparisons with the Benjamini, Krieger, and Yekutieli method; \*  $p < 0.05$ , \*\*  $p < 0.01$ , \*\*\*  $p < 0.001$ ).

To focus our analyses on foci of meningeal inflammation specifically, we performed unbiased UMAP clustering on the spatial transcriptomic dataset and identified 11 distinct clusters (Figure 3A). Grouping the dimensional reduction UMAP plot by EAE and naïve revealed that cluster eleven (C11) was restricted to EAE samples (Figure 3B). C11 makes up 1–5% of the total spots in those samples (Figure 3C), or about 20–120 total spots, and was significantly enriched in EAE relative to naïve samples (Figure 3D). Visualizing the clusters using spatial feature plots confirmed that most clusters map consistently to specific anatomic regions and were similar between naïve and EAE (Figure 3E; Supplementary Figure 3A). C11 overlapped with previously noted areas of meningeal MRI enhancement, suggesting that C11 represents areas of meningeal inflammation (Figure 3E; Supplementary Figure 3B–D). We compared the gene expression in C11 to other clusters and found 132 upregulated genes and 70 downregulated genes ( $p < 0.05$ ; Log2 fold change  $> 1$ ; Figure 3F). Inflammation-related genes were prominently represented in C11 relative to other clusters (Supplementary Table 2), with top genes including *Cd74*, *C3*, and *Gfap* (Figure 3G; Supplementary Figure 3E). We next performed gene set enrichment analysis of C11 spots using the Gene Ontology (GO) database<sup>22, 23</sup>, finding 538 variable gene sets (adjusted P-value  $< 0.05$ ; Supplementary Table 3). Among the most prominently enriched gene sets were those involved in antigen processing and presentation, complement activation, lymphocyte activation, and cytokine production and response (Figure 3H).

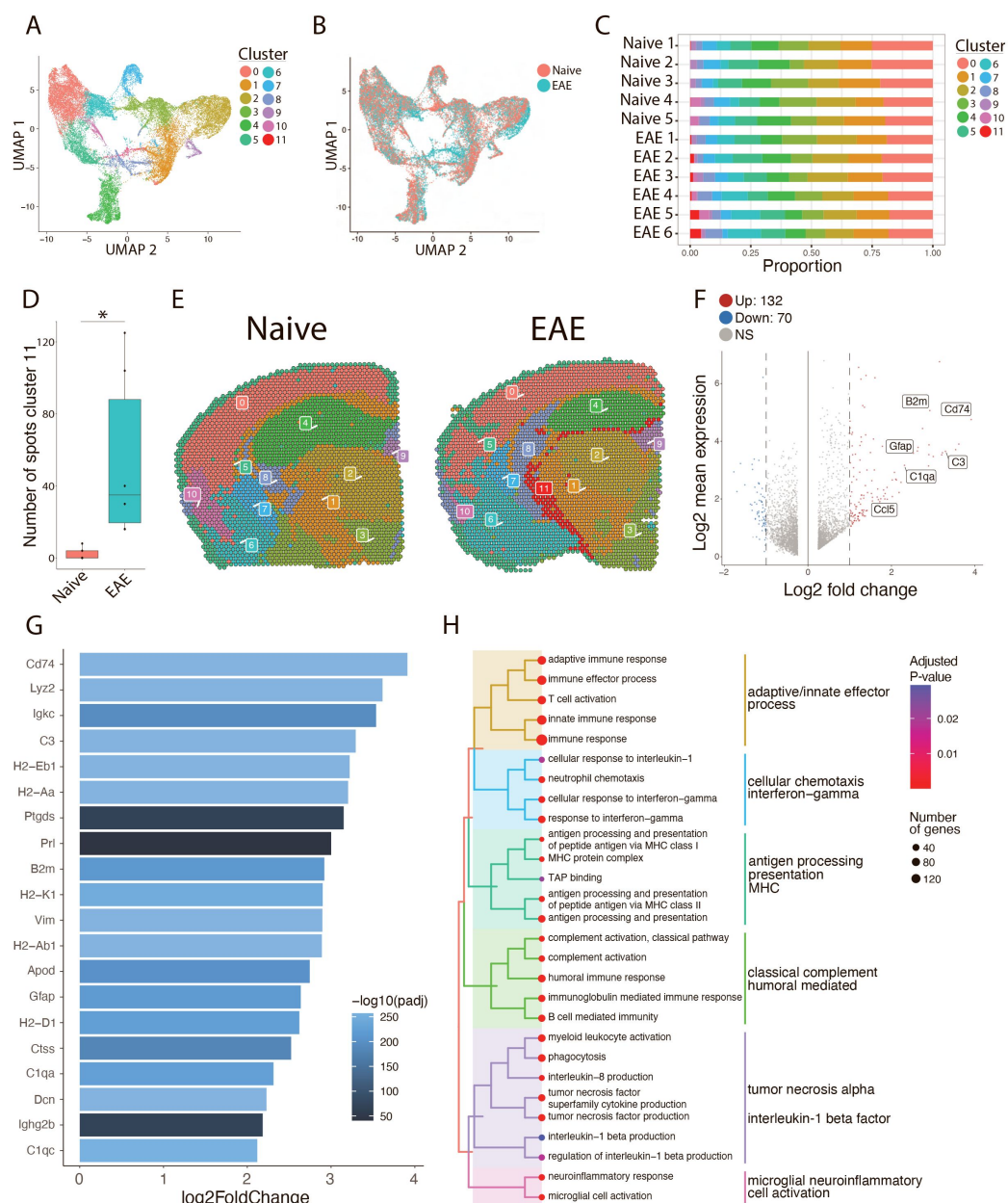


**Figure 3:**

## Unbiased clustering reveals a group of spots enriched in inflammatory genes.

(A–B) UMAP dimensionality reduction plots colored by (A) cluster or (B) group. (C) Bar plot showing the proportion of spots in each cluster by sample. (D) Number of spots in cluster 11 by group (N = 11; Student’s two-tailed T test). (E) Representative spatial feature plots of naïve and EAE samples showing the spatial distribution of each cluster. (F) MA plot comparing differences in gene expression between cluster 11 and all other clusters averaged across samples. Red and blue spots represent genes in cluster 11 that are significantly increased or decreased, respectively (adjusted p-value < 0.05, log<sub>2</sub> fold change > 1). (G) Bar plot of top 15 genes enriched in cluster 11 compared to other clusters. (H) Tree plot displaying gene set enrichment results using the gene ontology (GO) database. Spots in cluster 11 were compared to other spots and gene set sizes ranging from 10–500 were included (adjusted p-value < 0.05).

After establishing the defining transcriptomic features of meningeal inflammation in our model, we next sought to characterize inflammatory changes in the adjacent CNS parenchyma. We performed unbiased sub-clustering of each cluster in turn and found EAE-specific subclusters and differentially expressed genes within clusters 1 and 2. These subclusters were labelled 1\_3, 1\_4, and 2\_6 (Figure 4A-B; Supplemental Figure 4) and represent regions of the thalamus and hypothalamus (Figure 4C).

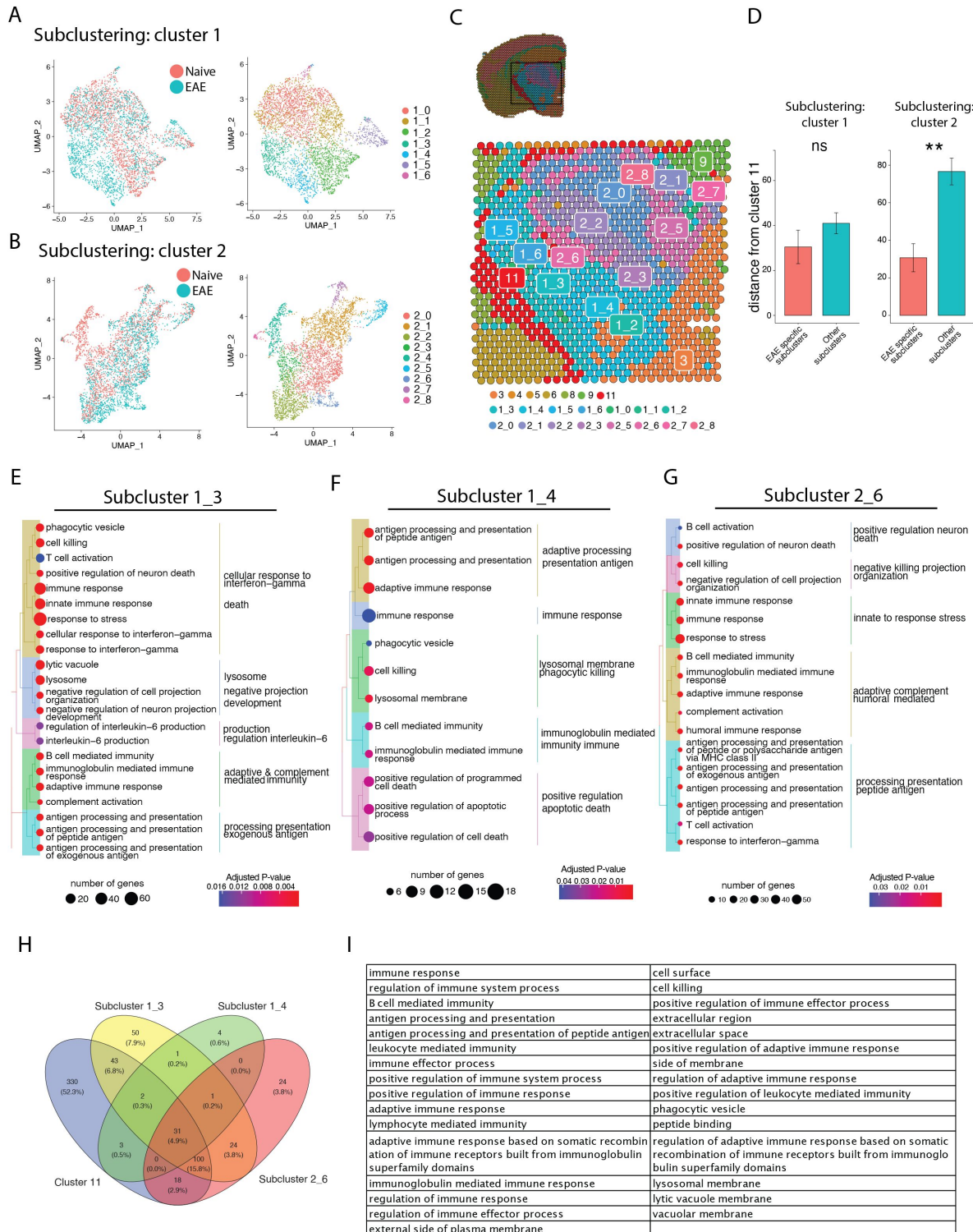




**Figure 4:**

## Subclustering of spots adjacent to meningeal immune follicles reveals a subset of active immune patterns.

(A) UMAP dimensionality reduction plots showing subclustering of cluster 1 colored by (top) group or (bottom) cluster. (B) UMAP dimensionality reduction plots showing subclustering of cluster 2 colored by (top) group or (bottom) cluster. (C) Representative spatial feature plot showing the locations of cluster 1 and 2 subclusters. (D) Distance from the center of indicated subclusters to the nearest point of cluster 11 ( $N = 11$ ; Student's two-tailed T-Test). (E–G) Tree plot displaying gene set enrichment results using the gene ontology (GO) database for subcluster 2\_6 (E), 1\_3 (F), and 1\_4 (G) compared to other spots in their respective clusters. (H) Venn diagram shows overlap of significantly enriched GO gene sets between cluster 11 and subclusters 1\_3, 1\_4, and 2\_6, with (I) 31 gene sets elevated in all. GO gene set of size ranging from 10–500 were included (adjusted  $p$ -value  $< 0.05$ ).

Next, we assessed whether EAE-specific subclusters were physically closer to meningeal inflammation than other related subclusters. The distance between the average location in each subcluster to the nearest point of C11 was calculated. In the subclusters of cluster 1, we found no difference in proximity to C11 between EAE-specific subclusters vs. subclusters present in EAE and naïve. However, in subclusters of cluster 2, the EAE-specific subcluster was significantly closer to C11 on average compared to other subclusters (Figure 4D). To explore which pathways were activated in these subclusters, we performed gene set enrichment analysis using the GO database (Figure 4E–G; Supplementary Tables 4–6). Overall, 31 upregulated pathways were conserved between cluster 11 and subclusters 1\_3, 1\_4, 2\_6 (Figure 4H). We found prominent conserved upregulation of pathways related to adaptive/B-cell mediated immunity, antigen processing and presentation, cell killing, and others (Figure 4I).

Our pathway analysis of meningeal inflammation and areas of inflamed adjacent brain parenchyma suggested that inflammatory signals increased in meningeal inflammation could have variable ‘penetration’ into the adjacent brain. We sought to test this using spatial trajectory gene/gene set expression modelling available within the SPATA2 software package<sup>20</sup>. Trajectories were drawn in EAE samples from the largest region of meningeal inflammation to the central thalamus (Figure 5A). Gene and gene set expression levels were then evaluated along the length of these trajectories and compared to ideal patterns of expression, as demonstrated for representative genes *B2m* and *C3* (Figure 5B–E). The difference between gene or gene set expression and the ideal patterns, here “logarithmic descending” or “gradient descending”, is represented by the residual line (Figures 5B, 5E). The area under the residual curve (residual AUC) is therefore inversely proportional to fit for the given gene or gene set and ideal pattern. *C3* expression declines rapidly along the trajectory and the logarithmic descending residual AUC is lower than gradient descending residual AUC (Figure 5E), while *B2m* follows a less steep decline and fits the two patterns similarly (Figure 5C). Trajectory analysis of gene sets enriched in meningeal inflammation and adjacent brain parenchyma was performed in this way, and the average residual AUC was calculated for gradient descending/ascending and logarithmic descending/ascending patterns (Figure 5Fi). As expected, all gene sets fit descending patterns better than ascending ones. There was variability in fit to the gradient descending pattern of expression, representing a more gradual decline in pathway enrichment along the trajectory, with gene sets related to antigen processing and presentation, cell killing, interleukin 6 production, and interferon gamma response having the best fit (Figure 5Fi). Enrichment score trajectory heatmap of a representative sample corroborates this, showing increased activity farther along the spatial trajectory for these gene sets (Figure 5Fii).

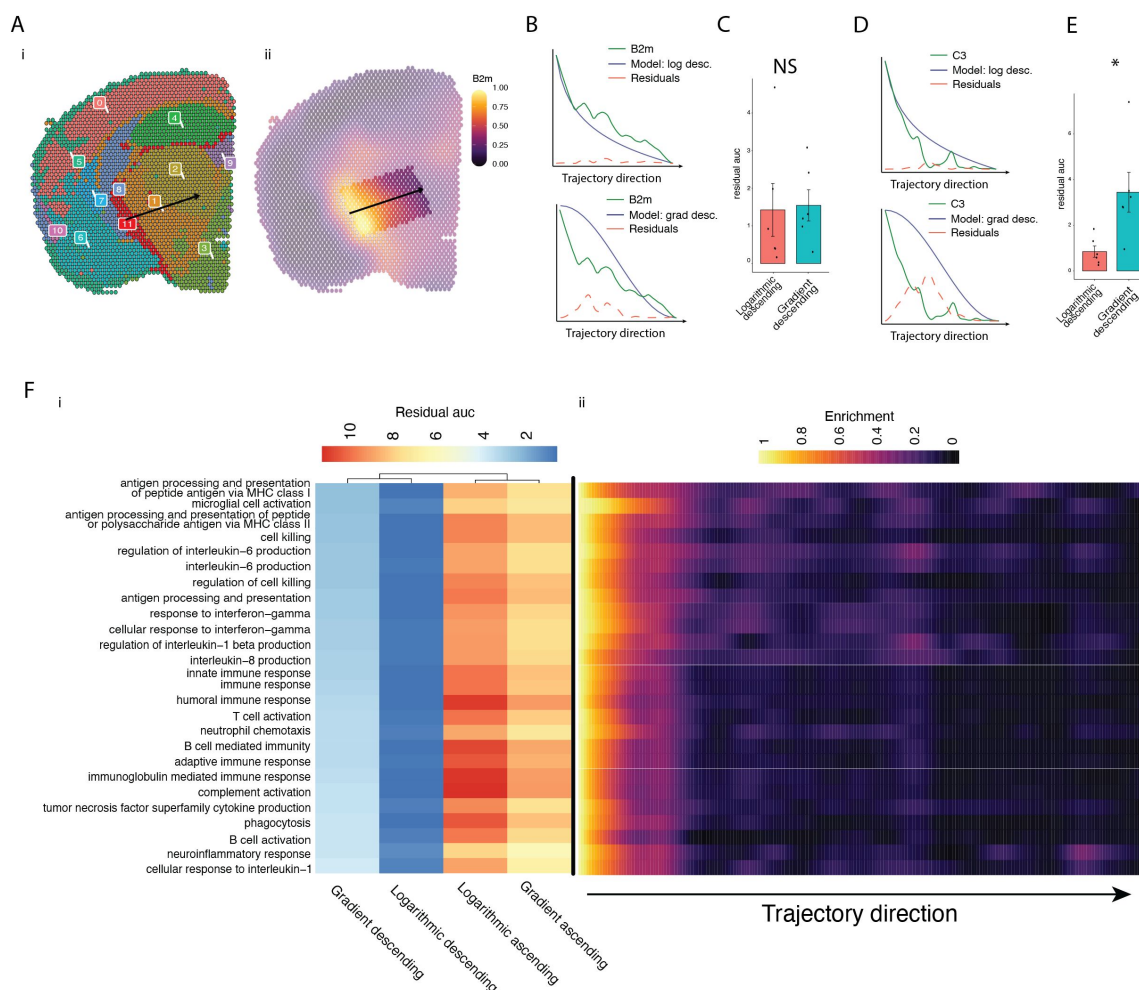


**Figure 5**

## Trajectory analysis reveals gradients of gene expression originating from meningeal lymphoid follicles.

(A) Trajectories were drawn based on spatial cluster plot (i) from C11 to C2 (ii). (B) Representative plot of *B2m* relative expression along the trajectory length. Green line: *B2m* expression; black line: ideal model fit, “logarithmic descending” (top) or “gradient descending” (bottom); red line: residual area under the curve (AUC) representing the difference between *B2m* expression and the ideal model. (C) Barplot showing residual AUC of *B2m* relative expression along the trajectory direction compared to “logarithmic descending” or “gradient descending” (Student’s two-tailed T-test). (D) Representative plot of *C3* relative expression along the trajectory length. Green line: *C3* expression; black line: ideal model fit, “logarithmic descending” (top) or “gradient descending” (bottom); red line: residual area under the curve (auc) representing the difference between *C3* expression and the ideal model. (E) Barplot showing residual AUC of *C3* relative expression along the trajectory direction compared to “logarithmic descending” or “gradient descending” (Student’s T-test). (F) Genesets that were previously identified as significantly enriched in C11 were selected for trajectory analysis. Residual AUCs were calculated for “logarithmic descending”, “gradient descending”, “logarithmic ascending”, and “gradient ascending” ideal fits and displayed on (i) a heatmap sorted by “gradient descending”. (ii) Representative feature plot demonstrating deeper penetration of upper genesets (related to antigen presentation and processing, microglial activation, IL-6 production, interferon gamma) response relative to other gene sets (B cell activation, T cell activation, TNF production, complement, humoral immune response).

## Discussion

Meninges-restricted inflammation in MS is intimately related to subpial grey matter demyelination<sup>3</sup>, atrophy, and neurocognitive symptoms, but therapeutically targeting this aspect of the disease is challenging due to poorly understood pathologic mechanisms. Here, we present spatial transcriptomics analysis in a mouse model of LMI, finding a broad swath of inflammatory pathways upregulated at foci of LMI and a subset of them upregulated in the nearby brain parenchyma. Notably, genes related to B cell mediated responses and antigen processing and presentation were upregulated in inflammatory parenchymal subclusters. Variable penetrance of inflammatory pathway activity was evident when analyzing genesets' expression pattern along a linear trajectory from LMI into the CNS parenchyma, where antigen processing and presentation, interleukin 6 production, and the IFN $\gamma$  response pathway activity followed a more gradual decline as compared to other pathways.

Prior work supports roles for pathways identified in our dataset, including B cell and IFN $\gamma$  mediated responses, in contributing to neurodegeneration in MS. LMI in MS is rich in B cells, and the critical role of B cells in MS has been underscored by the success of B cell depletion in relapsing and progressive MS. Recent studies have proposed numerous mechanisms whereby B cells could contribute to cortical pathology, including indirectly through activation and inflammatory polarization of T cells, myeloid cells, and astrocytes or directly through production of neurotoxic cytokines or antibodies<sup>28</sup>. B cell culture supernatants from MS patients, but not healthy controls, are toxic to rat and human neurons and oligodendrocytes with this effect being mediated by the extracellular vesicle (EV) fraction of the supernatants<sup>29, 30</sup>. B cells are also sources for inflammatory cytokines, such as IL-6 and GM-CSF, and antibodies, which are speculated to contribute to GMP<sup>28</sup>.

The role of IFN $\gamma$  in the pathogenesis of MS and EAE is complex, and likely has stage specific protective and pathologic effects<sup>31</sup>. Its prominent upregulation in EAE was initially considered evidence of its pathogenic nature, but subsequent experiments showed that it was pathogenic during the initiation phase but protective later in the course<sup>31</sup>. IFN $\gamma$  signaling and subsequent upregulation of antigen processing and presentation on glia has been identified as a mechanism that could lead to remyelination failure and subsequent neuronal loss<sup>32</sup>. Oligodendrocyte precursor cells (OPCs) upregulate antigen presentation and cross-presentation pathways in response to IFN $\gamma$ , promoting inflammation and making them susceptible to CD8<sup>+</sup> T cell killing<sup>32</sup>. Upregulation of genes for self-antigen presentation has also been noted in neurons and oligodendrocyte lineage (OL) cells in post-mortem MS single nucleus RNAseq<sup>33</sup>, and OL cells in EAE<sup>34, 35</sup>.

While SJL EAE models many features of LMI in MS<sup>18</sup>, it has several important limitations. The majority of LMI identified in mice with SJL EAE in our experiments occurred in subarachnoid cisterns, and as a result prominently affected areas of parenchyma including thalamus and hypothalamus as opposed to cortical lesions typically seen in MS. Interestingly, neuronal loss in the thalamus and other deep grey nuclei does occur in MS with a similar 'surface-in' gradient of neuronal injury, thought to also be related to toxic CSF-derived factors<sup>36, 37</sup>. We also noted some variability in the extent and location of LMI, which is unavoidable in EAE. While other animal models of LMI, such as directly injecting inflammatory cytokines into the meninges/cortex, produce more predictable regions of LMI, they involve traumatic injury to the brain and typically lack follicle-like structures<sup>38</sup>.

This work is the first to characterize a mouse model of LMI and grey matter injury using spatial transcriptomics, and in addition to the analysis presented here contributes a publicly available dataset for future research. We highlight the importance of antigen processing and

presentation and B cell mediated inflammation, which are prominently upregulated in sub-pial grey matter, in our model. Future studies should focus on spatial transcriptomics in post-mortem or biopsied human tissue. While access to appropriate samples remains a significant barrier, recent advances in RNA extraction from formalin fixed paraffin embedded tissues<sup>39, 40</sup> will allow for the use of large banks of historically collected and preserved samples and could dramatically improve availability.

## Acknowledgements

We thank members of the Calabresi lab for their valuable comments during multiple discussions of this work. We thank the Johns Hopkins Medicine Single Cell and Transcriptomics Core for their assistance with planning and data acquisition. We acknowledge the contribution of animals used in this research study.

## Ethics approval and consent to participate

All animal studies followed national and institutional guidelines for human animal treatment in compliance with the Johns Hopkins ACUC.

## Availability of data and material

Data availability: spatial transcriptomic data presented in this study will be made publicly available on the Gene Expression Omnibus (<https://www.ncbi.nlm.nih.gov/geo/>) at the time of publication.

## Competing interests

The authors have no competing interests to disclose.

## Funding

This work was supported in part by an investigator-initiated grant from EMD-Serono to PB, a Harry Weaver Neuroscience Scholar award to PB and a fellowship grant from the National Multiple Sclerosis Society and the American Brain Foundation (FAN- 2106-37832) to SPG.

## Authors' contributions

SPG, SK, SS, MS, PAC, and PB conceived and designed the experiments. SK, SS, and MS performed the experiments and collected the data. SPG and MS analyzed the data. SPG, SS, PAC, and PB wrote the manuscript. All authors reviewed and suggested improvements to the manuscript.



## Supplemental Figure 1

**Contrast enhancing meningeal inflammation in SJL EAE does not change at chronic time points or with clinical disease scores.** (A) Box plot of lesion number versus week post immunization. ANOVA with Tukey's HSD post-hoc test. (B) lesion number plotted against EAE score demonstrates no strong correlation ( $R^2 < 0.4$  in all cases).  $N = 16$ , data is representative of three pooled experiments.

## Supplemental Figure 2

**Quality control analysis of spatial transcriptomic data.** (A) Density of read counts, (B) number of unique molecular identifiers (UMI), (C) and the ratio of read count/UMI per spot for naïve and EAE samples. Most spots had  $> 500$  read count (A),  $> 250$  UMI (B), and  $> 0.80$   $\log(\text{nCount}/\text{UMI})$  (C). (D) Dot plot shows most spots having linear correlation between UMI and read count. (E-F) Violin plots of read counts (E) and UMI (F) per sample. (G-H) Representative spatial feature plots of read count (F) and UMI (G) demonstrate expected anatomic variability in transcript amount and diversity. (I-J) UMAP dimensionality reduction plots, colored by mouse (I) or slide (J). (K) MA plot of genes enriched in EAE compared to naïve samples. Data was pseudobulked by sample and groups were compared using DESeq2 for gene enrichment (adjusted p-value  $< 0.05$ ,  $\log_2$  fold change  $> 1$ ).

## Supplementary Figure 3

**Spatial and transcriptional properties of inflammatory clusters.** (A) Representative spatial feature plots of naïve (top row) and EAE (bottom row) samples colored by cluster show consistent labeling of anatomic regions and the distribution of meningeal inflammation (cluster 11). (B-D) Representative images of gadolinium enhanced MRI scans collected 10 weeks after immunizations and samples collected from the same animal. Areas of meningeal enhancement (red arrows) correlate with cluster 11. (E) Dot plot of the top 100 significantly enriched genes (sorted by adjusted P value) in cluster 11 compared to other clusters. Dot color represents expression value and dot size represents the percent of spots within that cluster expressing the gene.

## Supplementary Figure 4

**Subcluster analysis reveals EAE-specific subclusters and gene enrichment.** (A-K) Data from each individual cluster was extracted and unbiased subclustering performed based on gene expression. UMAP plots are shown colored by subcluster (left panel) and group (middle panel). Data from each cluster was isolated, pseudobulked by sample, and groups were compared using DESeq2 for gene enrichment (right panel; adjusted p-value  $< 0.05$ ,  $\log_2$  fold change  $> 1$ ). EAE specific subclusters and enriched genes were identified in Clusters 1 (B) and 2 (C).

## References

1. Reich D. S. , Lucchinetti C. F. , Calabresi P. A. (2018) **Multiple Sclerosis** *New England Journal of Medicine* **378**:169–180
2. Faissner S. , Plemel J. R. , Gold R. , Yong V. W (2019) **Progressive multiple sclerosis: from pathophysiology to therapeutic strategies** *Nat Rev Drug Discov* **18**:905–922
3. Howell O. W. , et al. (2011) **Meningeal inflammation is widespread and linked to cortical pathology in multiple sclerosis** *Brain* **134**:2755–2771
4. Absinta M. , et al. (2015) **Gadolinium-based MRI characterization of leptomeningeal inflammation in multiple sclerosis** *Neurology* **85**:18–28
5. Wicken C. , Nguyen J. , Karna R. , Bhargava P (2018) **Leptomeningeal inflammation in multiple sclerosis: Insights from animal and human studies** *Multiple Sclerosis and Related Disorders* **26**:173–182
6. Geurts J. J. , Barkhof F (2008) **Grey matter pathology in multiple sclerosis** *The Lancet Neurology* **7**:841–851
7. Bø L. , Vedeler C. A. , Nyland H. I. , Trapp B. D. , Mørk S. J (2003) **Subpial Demyelination in the Cerebral Cortex of Multiple Sclerosis Patients** *J Neuropathol Exp Neurol* **62**:723–732
8. Magliozzi R. , et al. (2010) **A Gradient of neuronal loss and meningeal inflammation in multiple sclerosis** *Ann Neurol* **68**:477–493
9. Mainero C. , et al. (2015) **A gradient in cortical pathology in multiple sclerosis by in vivo quantitative 7 T imaging** *Brain* **138**:932–945
10. van Horssen J. , Brink B. P. , de Vries H. E. , van der Valk P. , Bø L (2007) **The Blood-Brain Barrier in Cortical Multiple Sclerosis Lesions** *J Neuropathol Exp Neurol* **66**:321–328
11. Bø L. , Vedeler C. A. , Nyland H. , Trapp B. D. , Mørk S. J (2003) **Intracortical multiple sclerosis lesions are not associated with increased lymphocyte infiltration** *Mult Scler* **9**:323–331
12. Pikor N. B. , Prat A. , Bar-Or A. , Gommerman J. L (2016) **Meningeal Tertiary Lymphoid Tissues and Multiple Sclerosis: A Gathering Place for Diverse Types of Immune Cells during CNS Autoimmunity** *Front Immunol* **6**
13. Magliozzi R. , et al. (2018) **Inflammatory intrathecal profiles and cortical damage in multiple sclerosis: Intrathecal Inflammation in MS** *Ann Neurol* **83**:739–755
14. Magliozzi R. , et al. (2019) **Meningeal inflammation changes the balance of TNF signalling in cortical grey matter in multiple sclerosis** *Journal of Neuroinflammation* **16**

15. Storch M. K. , et al. (2006) **Cortical demyelination can be modeled in specific rat models of autoimmune encephalomyelitis and is major histocompatibility complex (MHC) haplotype-related** *J Neuropathol Exp Neurol* **65**:1137–1142
16. Merkler D. , et al. (2006) **Myelin oligodendrocyte glycoprotein-induced experimental autoimmune encephalomyelitis in the common marmoset reflects the immunopathology of pattern II multiple sclerosis lesions** *Mult Scler* **12**:369–374
17. Brink B. P. , et al. (2005) **The pathology of multiple sclerosis is location-dependent: no significant complement activation is detected in purely cortical lesions** *J Neuropathol Exp Neurol* **64**:147–155
18. Magliozzi R. , Columba-Cabezas S. , Serafini B. , Aloisi F (2004) **Intracerebral expression of CXCL13 and BAFF is accompanied by formation of lymphoid follicle-like structures in the meninges of mice with relapsing experimental autoimmune encephalomyelitis** *J Neuroimmunol* **148**:11–23
19. Bhargava P. , et al. (2021) **Imaging meningeal inflammation in CNS autoimmunity identifies a therapeutic role for BTK inhibition** *Brain* **144**:1396–1408
20. Kueckelhaus J. , et al. (2020) **Inferring spatially transient gene expression pattern from spatial transcriptomic studies**  
<https://doi.org/10.1101/2020.10.20.346544>
21. Hafemeister C. , Satija R (2019) **Normalization and variance stabilization of single-cell RNA- seq data using regularized negative binomial regression** *Genome Biology* **20**
22. Gene Ontology Consortium (2021) **The Gene Ontology resource: enriching a GOLD mine** *Nucleic Acids Res* **49**:D325–D334
23. Ashburner M. , et al. (2000) **Gene ontology: tool for the unification of biology. The Gene Ontology Consortium** *Nat Genet* **25**:25–29
24. Wu T. , et al. (2021) **clusterProfiler 4.0: A universal enrichment tool for interpreting omics data** *The Innovation* **2**
25. Schubert M. , et al. (2018) **Perturbation-response genes reveal signaling footprints in cancer gene expression** *Nat Commun* **9**
26. Benjamini Y. , Hochberg Y (1995) **Controlling the False Discovery Rate: A Practical and Powerful Approach to Multiple Testing** *Journal of the Royal Statistical Society: Series B (Methodological)* **57**:289–300
27. Bedussi B. , et al. (2017) **Paravascular channels, cisterns, and the subarachnoid space in the rat brain: A single compartment with preferential pathways** *J Cereb Blood Flow Metab* **37**:1374–1385

28. Bhargava P. , Hartung H.-P. , Calabresi P. A (2022) **Contribution of B cells to cortical damage in multiple sclerosis** *Brain* **145**:3363–3373
29. Lisak R. P. , et al. (2017) **B cells from patients with multiple sclerosis induce cell death via apoptosis in neurons in vitro** *Journal of Neuroimmunology* **309**:88–99
30. Benjamins J. A. , et al. (2019) **Exosome-enriched fractions from MS B cells induce oligodendrocyte death** *Neurology - Neuroimmunology Neuroinflammation* **6**
31. Arellano G. , Ottum P. A. , Reyes L. I. , Burgos P. I. , Naves R (2015) **Stage-Specific Role of Interferon-Gamma in Experimental Autoimmune Encephalomyelitis and Multiple Sclerosis** *Front. Immunol* **6**
32. Kirby L. , et al. (2019) **Oligodendrocyte precursor cells present antigen and are cytotoxic targets in inflammatory demyelination** *Nature Communications* **10**
33. Schirmer L. , et al. (2019) **Neuronal vulnerability and multilineage diversity in multiple sclerosis** *Nature* **573**:75–82
34. Falcão A. M. , et al. (2019) **Disease-specific oligodendrocyte lineage cells arise in multiple sclerosis** *Nat Med* **24**:1837–1844
35. Jäkel S. , et al. (2019) **Altered human oligodendrocyte heterogeneity in multiple sclerosis** *Nature* **566**:543–547
36. Azevedo C. J. , et al. (2018) **Thalamic Atrophy in Multiple Sclerosis: A Magnetic Resonance Imaging Marker of Neurodegeneration throughout Disease** *Ann Neurol* **83**:223–234
37. Magliozzi R. , et al. (2022) **“Ependymal-in” Gradient of Thalamic Damage in Progressive Multiple Sclerosis** *Annals of Neurology* **92**:670–685
38. Silva B. A. , Miglietta E. , Ferrari C. C (2021) **Neuroinflammation in cortical and meningeal pathology in multiple sclerosis: understanding from animal models** *Neuroimmunology and Neuroinflammation* **8**:174–184
39. Newton Y. , et al. (2020) **Large scale, robust, and accurate whole transcriptome profiling from clinical formalin-fixed paraffin-embedded samples** *Sci Rep* **10**
40. Gracia Villacampa E. , et al. (2021) **Genome-wide spatial expression profiling in formalin-fixed tissues** *Cell Genomics* **1**

## Author information

### Sachin P. Gadani

Division of Neuroimmunology, Department of Neurology, Johns Hopkins University School of Medicine, Baltimore, MD, USA



**Saumitra Singh**

Division of Neuroimmunology, Department of Neurology, Johns Hopkins University School of Medicine, Baltimore, MD, USA

**Sophia Kim**

Division of Neuroimmunology, Department of Neurology, Johns Hopkins University School of Medicine, Baltimore, MD, USA

**Matthew D. Smith**

Division of Neuroimmunology, Department of Neurology, Johns Hopkins University School of Medicine, Baltimore, MD, USA

ORCID iD: [0000-0001-6614-569X](https://orcid.org/0000-0001-6614-569X)

**Peter A. Calabresi**

Division of Neuroimmunology, Department of Neurology, Johns Hopkins University School of Medicine, Baltimore, MD, USA, Solomon Snyder, Department of Neuroscience Johns Hopkins University School of Medicine, Baltimore, MD, USA

**Pavan Bhargava**

Division of Neuroimmunology, Department of Neurology, Johns Hopkins University School of Medicine, Baltimore, MD, USA

**For correspondence:** [pbharg2@jhmi.edu](mailto:pbharg2@jhmi.edu)

ORCID iD: [0000-0002-7947-9418](https://orcid.org/0000-0002-7947-9418)

**Editors**

Reviewing Editor

**Irene Salinas**

University of New Mexico, United States of America

Senior Editor

**Satyajit Rath**

Indian Institute of Science Education and Research (IISER), India

**Reviewer #1 (Public Review):**

Multiple sclerosis (MS) is a debilitating autoimmune disease that causes loss of myelin in neurons of the central nervous system. MS is characterized by the presence of inflammatory immune cells in several brain regions as well as the brain barriers (meninges). This study aims to understand the local immune hallmarks in regions of the brain parenchyma that are adjacent to the leptomeninges in a mouse model of MS. The leptomeninges are known to be a foci of inflammation in MS and perhaps "bleed" inflammatory cells and molecules to adjacent brain parenchyma regions. To do so, they use novel technology called spatial transcriptomics so that the spatial relationships between the two regions remain intact. The study identifies canonical inflammatory genes and gene sets such as complement and B cells enriched in the parenchyma in close proximity to the leptomeninges in the mouse model of MS but not control. The manuscript is very well written and easy to follow. The results will become a useful resource to others working in the field and can be followed by time series experiments where the same technology can be applied to the different stages of the disease.

## Reviewer #2 (Public Review):

Accumulating data suggests that the presence of immune cell infiltrates in the meninges of the multiple sclerosis brain contributes to the tissue damage in the underlying cortical grey matter by the release of inflammatory and cytotoxic factors that diffuse into the brain parenchyma. However, little is known about the identity and direct and indirect effects of these mediators at a molecular level. This study addresses the vital link between an adaptive immune response in the CSF space and the molecular mechanisms of tissue damage that drive clinical progression. In this short report the authors use a spatial transcriptomics approach using Visium Gene Expression technology from 10x Genomics, to identify gene expression signatures in the meninges and the underlying brain parenchyma, and their interrelationship, in the PLP-induced EAE model of MS in the SJL mouse. MRI imaging using a high field strength (11.7T) scanner was used to identify areas of meningeal infiltration for further study. They report, as might be expected, the upregulation of genes associated with the complement cascade, immune cell infiltration, antigen presentation, and astrocyte activation. Pathway analysis revealed the presence of TNF, JAK-STAT and NFkB signaling, amongst others, close to sites of meningeal inflammation in the EAE animals, although the spatial resolution is insufficient to indicate whether this is in the meninges, grey matter, or both.

UMAP clustering illuminated a major distinct cluster of upregulated genes in the meninges and smaller clusters associated with the grey matter parenchyma underlying the infiltrates. The meningeal cluster contained genes associated with immune cell functions and interactions, cytokine production, and action. The parenchymal clusters included genes and pathways related to glial activation, but also adaptive/B-cell mediated immunity and antigen presentation. This again suggests a technical inability to resolve fully between the compartments as immune cells do not penetrate the pial surface in this model or in MS. Finally, a trajectory analysis based on distance from the meningeal gene cluster successfully demonstrated descending and ascending gradients of gene expression, in particular a decline in pathway enrichment for immune processes with distance from the meninges.

Although these results confirm what we already know about processes involved in the meninges in MS and its models and gradients of pathology in sub-pial regions, this is the first to use spatial transcriptomics to demonstrate such gradients at a molecular level in an animal model that demonstrates lymphoid like tissue development in the meninges and associated grey matter pathology. The mouse EAE model being used here does reproduce many, although not all, of the pathological features of MS and the ability to look at longer time points has been exploited well. However, this particular spatial transcriptomics technique cannot resolve at a cellular level and therefore there is a lot of overlap between gene expression signatures in the meninges and the underlying grey matter parenchyma.

The short nature of this report means that the results are presented and discussed in a vague way, without enough molecular detail to reveal much information about molecular pathogenetic mechanisms.

The trajectory analysis is a good way to explore gradients within the tissues and the authors are to be applauded for using this approach. However, the trajectory analysis does not tell us much if you only choose 2 genes that you think might be involved in the pathogenetic processes going on in the grey matter. It might be more useful to choose some genes involved in pathogenetic processes that we already know are involved in the tissue damage in the underlying grey matter in MS, for which there is already a lot of literature, or genes that respond to molecules we know are increased in MS CSF, although the animal models may be very different. Why were C3 and B2m chosen here?

**Strengths:**

- The mouse model does exhibit many of the features of the compartmentalized immune response seen in MS, including the presence of meningeal immune cell infiltrates in the central sulcus and over the surface of the cortex, with the presence of FDC's HEVs PNAd+ vessels and CXCL13 expression, indicating the formation of lymphoid like cell aggregates. In addition, disruption of the glia limitans is seen, as in MS. Increased microglial reactivity is also present at the pial surface.
- Spatial transcriptomics is the best approach to studying gradients in gene expression in both white matter and grey matter and their relationship between compartments.
- It would be useful to have more discussion of how the upregulated pathways in the two compartments fit with what we know about the cellular changes occurring in both, for which presumably there is prior information from the group's previous publications.

**Limitations:**

- EAE in the mouse is not MS and may be far removed when one considers molecular mechanisms, especially as MS is not a simple anti-myelin protein autoimmune condition. Therefore, this study could be following gene trajectories that do not exist in MS. This needs a significant amount of discussion in the manuscript if the authors suggest that it is mimicking MS.
- The model does not have the cortical subpial demyelination typical of MS and it is unknown whether neuronal loss occurs in this model, which is the main feature of cytokine-mediated neurodegeneration in MS. If it does not then a whole set of genes will be missing that are involved in the neuronal response to inflammatory stimuli that may be cytotoxic.
- Visium technology does not get down to single cell level and does not appear to allow resolution of the border between the meninges and the underlying grey matter.
- Neuronal loss in the MS cortex is independent of demyelination and therefore not related to remyelination failure. There does not appear to be any cortical grey matter demyelination in these animals, so it is difficult to relate any of the gene changes seen here to demyelination.
- No mention of how the ascending and descending patterns of gene expression may be due to the gradient of microglial activation that underlies meningeal inflammation, which is a big omission.

**Reviewer #3 (Public Review):**

In this study, Gadani et al. induced EAE in SJL/J mice and performed a comprehensive spatial transcriptomic analysis in areas of meningeal inflammation during the relapse phase of the disease. The authors found specific enrichment in spatial gene signatures (cluster 11) in the regions of increased contrast-enhancement by MRI (where meningeal extravasation of activated immune cells is observed) that overlap with signatures in the adjacent brain parenchyma, namely the thalamus. Several pathways were similarly upregulated in the meningeal-associated cluster 11 and adjacent parenchymal clusters (like adaptive mediated immunity, and antigen processing and presentation), suggestive of a "leakage" of inflammatory mediators from the meninges into the brain during the re-activation of disease. The tested hypothesis, as well as the data presented in this study, is quite interesting and novel.

**Author Response:**

We thank Reviewer #1 for their positive assessment of our work.

## Reviewer #2 (Public Review):

*[...] Although these results confirm what we already know about processes involved in the meninges in MS and its models and gradients of pathology in sub-pial regions, this is the first to use spatial transcriptomics to demonstrate such gradients at a molecular level in an animal model that demonstrates lymphoid like tissue development in the meninges and associated grey matter pathology. The mouse EAE model being used here does reproduce many, although not all, of the pathological features of MS and the ability to look at longer time points has been exploited well. However, this particular spatial transcriptomics technique cannot resolve at a cellular level and therefore there is a lot of overlap between gene expression signatures in the meninges and the underlying grey matter parenchyma.*

We appreciate the reviewer's concise summary and comments on our manuscript. We agree that the Visium spatial sequencing technology we applied is limited in its resolution and cannot precisely distinguish individual cells or anatomic regions. For that reason, there is undoubtedly some overlap between gene expression signatures in the meninges and underlying parenchyma, particularly in spots on the borders of the meningeal inflammation clusters. However, we believe that the majority of meningeal inflammation ("cluster 11") spots are indeed in the meninges and represent the spatial transcriptome of that niche. To support this, in the revised manuscript we will provide H&E images with the UMAP clusters overlaid to demonstrate the anatomic borders that correlate with the clusters.

*The short nature of this report means that the results are presented and discussed in a vague way, without enough molecular detail to reveal much information about molecular pathogenetic mechanisms.*

We thank the reviewer for this comment. The goal of this work is to transcriptomically characterize the spatial relationship between areas of meningeal inflammation and the underlying parenchyma. While we agree that mechanistic studies are needed to further evaluate the role of presented signaling pathways, those experiments are beyond the scope of this brief report.

*The trajectory analysis is a good way to explore gradients within the tissues and the authors are to be applauded for using this approach. However, the trajectory analysis does not tell us much if you only choose 2 genes that you think might be involved in the pathogenetic processes going on in the grey matter. It might be more useful to choose some genes involved in pathogenetic processes that we already know are involved in the tissue damage in the underlying grey matter in MS, for which there is already a lot of literature, or genes that respond to molecules we know are increased in MS CSF, although the animal models may be very different. Why were C3 and B2m chosen here?*

We appreciate the reviewer's points here. C3 and B2m were chosen as examples of genes that have differential fit to the gradient descending pattern to assist the reader in interpreting subsequent gene set trajectory analysis. However, we agree that there are many other genes of interest and will expand the number of genes displayed in our revised manuscript.

### *Strengths:*

- *The mouse model does exhibit many of the features of the compartmentalized immune response seen in MS, including the presence of meningeal immune cell infiltrates in the central sulcus and over the surface of the cortex, with the presence of FDC's HEVs PNAd+ vessels and CXCL13 expression, indicating the formation of lymphoid like cell aggregates. In addition, disruption of the glia limitans is seen, as in MS. Increased microglial reactivity is also present at the pial surface.*
- *Spatial transcriptomics is the best approach to studying gradients in gene expression in both*



*white matter and grey matter and their relationship between compartments.*

*- It would be useful to have more discussion of how the upregulated pathways in the two compartments fit with what we know about the cellular changes occurring in both, for which presumably there is prior information from the group's previous publications.*

*Limitations:*

*- EAE in the mouse is not MS and may be far removed when one considers molecular mechanisms, especially as MS is not a simple anti-myelin protein autoimmune condition.*

*Therefore, this study could be following gene trajectories that do not exist in MS. This needs a significant amount of discussion in the manuscript if the authors suggest that it is mimicking MS.*

*- The model does not have the cortical subpial demyelination typical of MS and it is unknown whether neuronal loss occurs in this model, which is the main feature of cytokine-mediated neurodegeneration in MS. If it does not then a whole set of genes will be missing that are involved in the neuronal response to inflammatory stimuli that may be cytotoxic.*

*- Visium technology does not get down to single cell level and does not appear to allow resolution of the border between the meninges and the underlying grey matter.*

*- Neuronal loss in the MS cortex is independent of demyelination and therefore not related to remyelination failure. There does not appear to be any cortical grey matter demyelination in these animals, so it is difficult to relate any of the gene changes seen here to demyelination.*

*- No mention of how the ascending and descending patterns of gene expression may be due to the gradient of microglial activation that underlies meningeal inflammation, which is a big omission.*

We thank the reviewer for their insightful comments on the strengths and limitations of our study. Regarding the SJL EAE model we use in this paper, it certainly is not a perfect model of meningeal inflammation in MS, indeed we believe that no such animal model exists, but it does recapitulate several key features of human disease as described by the reviewer. Spatial transcriptomics of cortical grey matter lesions and overlying meninges of samples derived from patients with MS would be ideal, though access to this tissue is highly limited. In the revised manuscript we will include more detailed discussion of the limitations in applying these findings to MS. However, in addition to potential implications for MS research, our data contribute more generally to understanding of meningeal inflammation and penetrance of inflammation into brain tissue.

We acknowledge that sub-pial neuronal loss has not been assessed in SJL EAE, and if present it would increase the relevance of this model to neurodegeneration. We are currently working to assess this.

We agree with the reviewer that Visium technology is limited in its ability to discriminate individual cells, as discussed above (2.2).

We agree that gene expression by activated microglia is likely a major driver of the transcriptomic changes observed in the parenchyma, and thank the reviewer for highlighting this. We will add discussion of this to our revised manuscript, and intend to generate additional data regarding the contribution of subpial microglial activation to the measured transcriptomic changes.

Finally, we thank Reviewer #3 for their assessment of our work.